Supporting information

The solvent engineering by ACN for the growth of high quality $CsPbBr_3$ single crystals

Kunpeng Mou[a], Xiaoxi Feng[b], Fangxiong Tang[b], Wenzhen Wang[c], Xudong Tang[b,d], Yongning Liu[a], Benlan Zeng[a], Sirui Bao[b], Minghao Cui[b,d], Jianing Hu[a], Huaxing Gou[a], Yan Zhu[a,*], Jinkun Liu[a], Run Xu[b,d,*]

[a] *Faculty of Materials Science and Technology, Kunming University of Science and Technology, Kunming 650093, China*

[b] *School of Materials Science and Engineering, Shanghai University, Shanghai 200444, China*

[c] *Shanghai Technical Institute of Electronics & Information, 3098 Wahong Road, Shanghai 201411, China*

[d] *Zhejiang Institute of Advanced Materials, Shanghai University, 1588 Huaxiang Street, Jiashan 314113, Zhejiang, China.*

* *Corresponding author:*
Yan Zhu (zhuyan@kust.edu.cn); Run Xu (runxu@staff.shu.edu.cn)

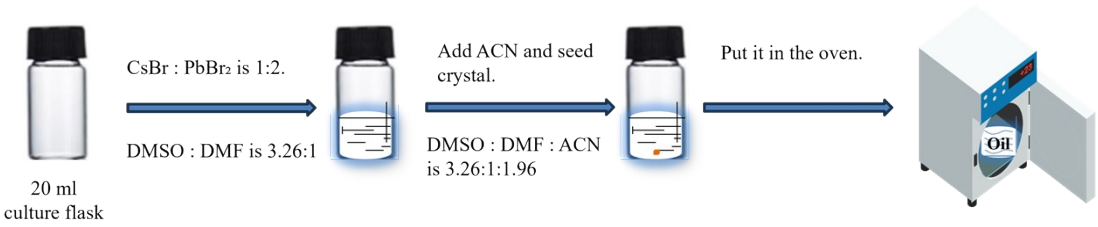

Fig.S1 Schematic diagram of the solution-growth process of $CsPbBr_3$ single crystal with ACN addition (molar ratios in the figure are indicated).

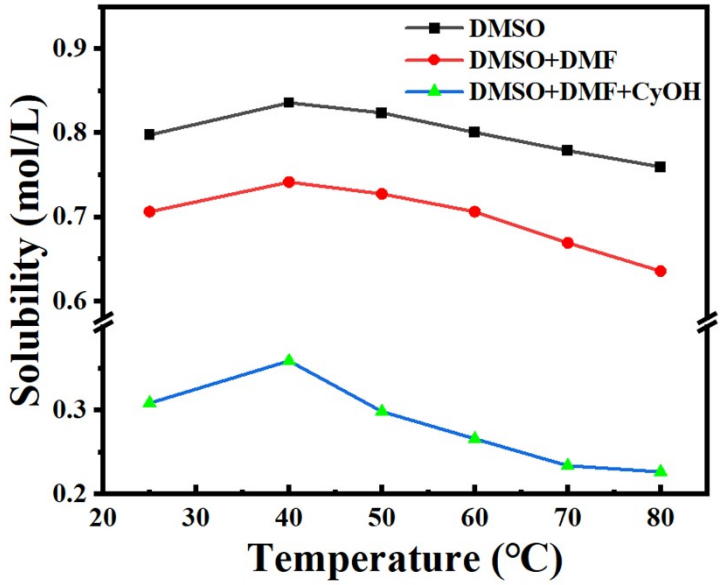

Fig. S2 Solubility curves of $CsPbBr_3$ in DMSO, DMSO/DMF, and DMSO/DMF/CyOH.

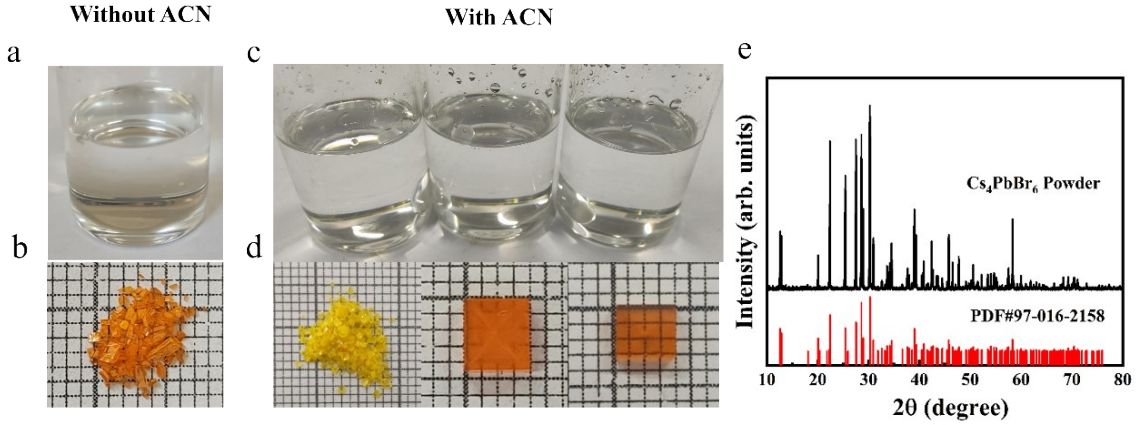

Fig. S3 (a) Precursor solution prepared using DMSO as the solvent. (b) Crystals grown from the solution in Fig. S2a. (c) Precursor solutions prepared using DMSO, a volume ratio of 4:1 of DMSO to DMF, and a volume ratio of 3:1 of DMSO to DMF as solvents. (d) Crystals have grown after adding ACN to each system in Fig. S2c. (e) Powder XRD characterization of the yellow-green crystals obtained using DMSO as the solvent and adding ACN as shown in Fig. S2d.

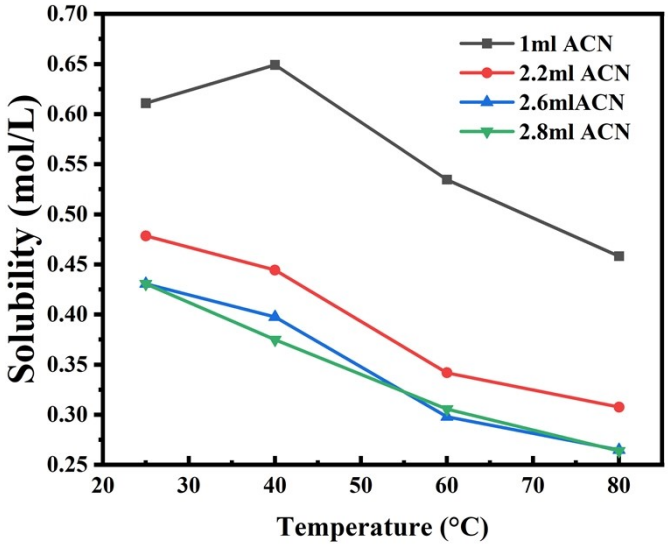

Fig. S4 The solubility curves of $CsPbBr_3$ under different ACN addition amounts.

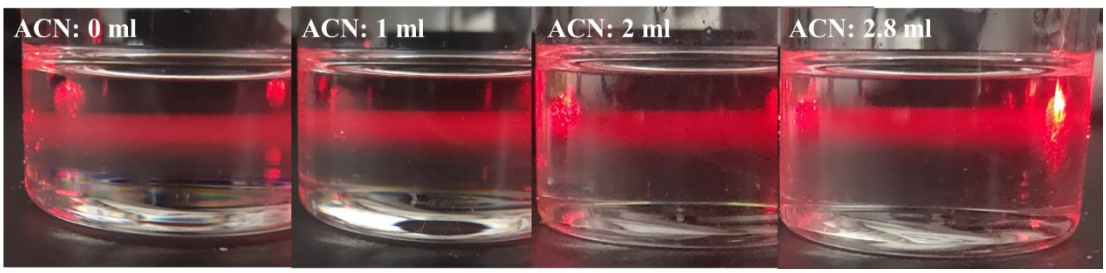

Fig. S5 Tyndall effect, in precursor solutions of the same concentration but with various amounts of ACN, respectively.

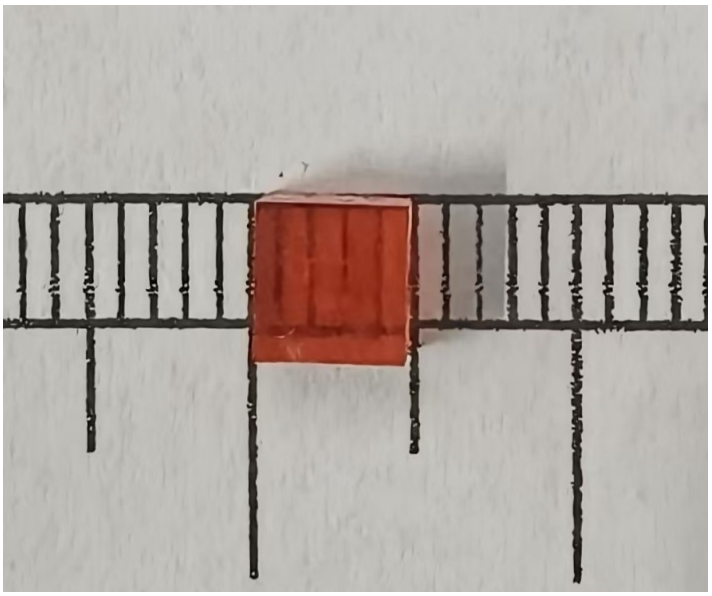

Fig. S6 Photograph of $CsPbBr_3$ crystals growing in the DMSO/DMF/CyOH solvent.

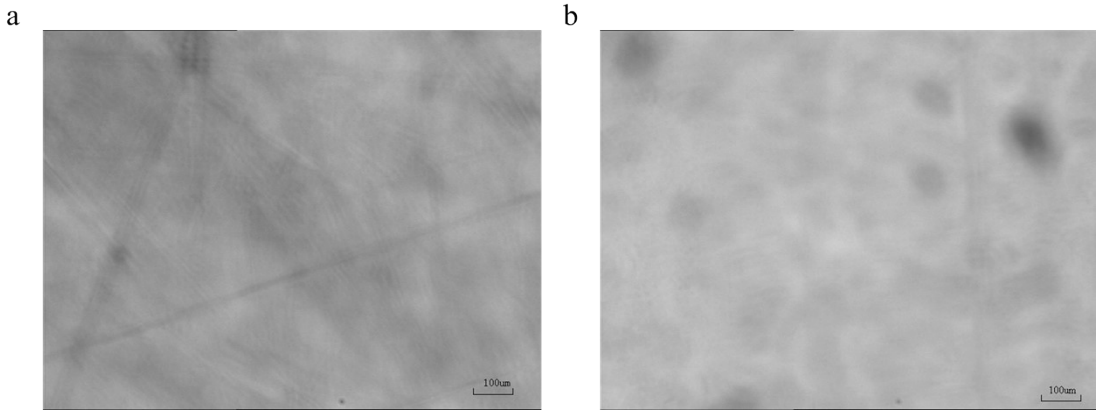

Fig. S7 (a) Infrared transmission images of $CsPbBr_3$ single crystal after polishing and (b) the same crystal after 8 months under a controlled environment (humidity < 40%).

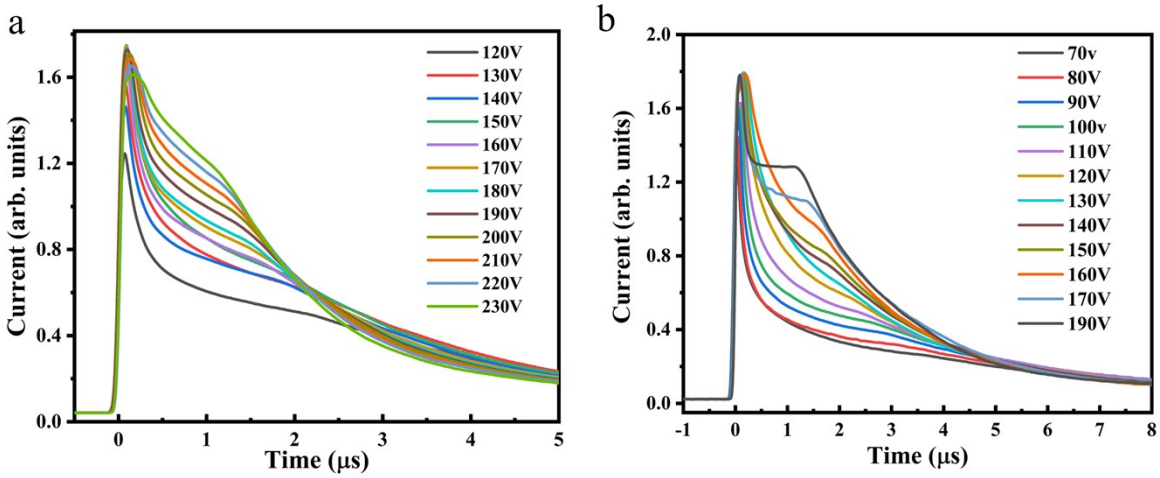

Fig. S8 (a) Electron and (b) Hole ToF spectra under different biases.

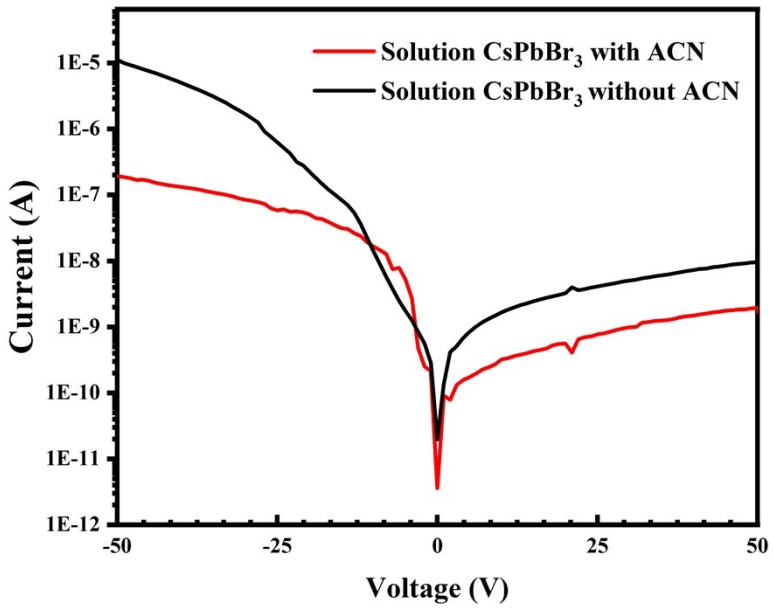

Fig. S9 The dark current of $CsPbBr_3$ crystals grown with and without ACN.

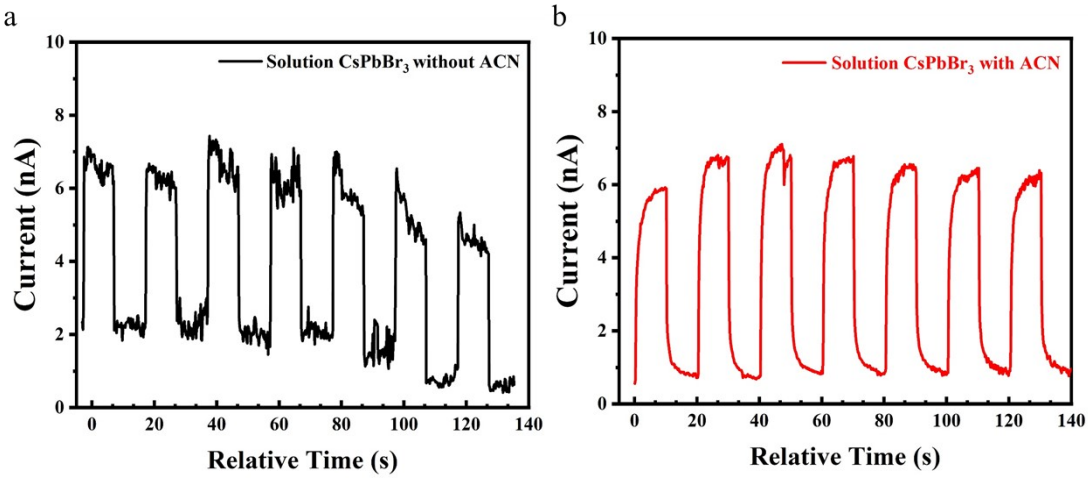

Fig. S10 X-ray response at a bias voltage of 5 V and an incident dose rate of 1.6 $\mu Gy^{-1} \cdot s^{-1}$.

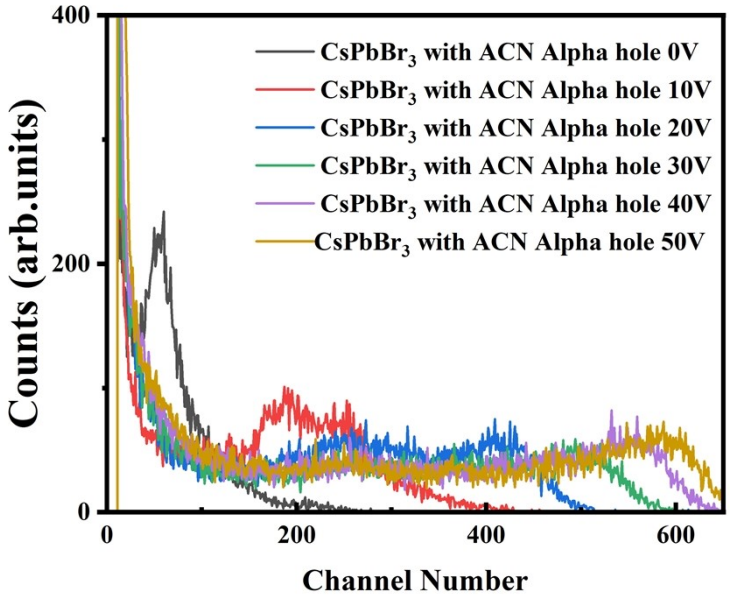

Fig. S11 Alpha-particle energy spectra irradiated by ^{241}Am under different biases.

Table S1 Summary of the growth of $CsPbBr_3$ single crystals.

Researcher	Solvent	Additives	Growth method	Growth temperature (°C)	XRC (°)	τ or μτ (ns or cm²/V)	Transmittance (%)
Sujith *et al.* [26]	DMSO	none	LTC[a]	27-30	none	none	none
Gao *et al.* [27]	DMSO	none	ITC[b]	110	none	τ2=17.03	none
Chen *et al.* [28]	DMSO	none	ITC[b]	140	0.043	none	none
Feng *et al.* [19]	DMSO	Choline Bromide	ITC[b]	80-85	none	$\mu\tau_e=1.80\times10^{-3}$	none
Pan *et al.* [29]	DMSO	TMAB	ITC[b]	60-85	none	$\tau_{ave}=88$	none
Dirin *et al.* [23]	DMSO/DMF/ CyOH	none	ITC[b]	90-110	none	$\mu\tau=2\times10^{-4}$	none
Zhang *et al.* [24]	DMSO/DMF/ CyOH	none	ITC[b]	49.5	none	$\tau_1=2.9$; $\tau_2=25.1$	74%
Cheng *et al.* [25]	DMSO/DMF/ CyOH	none	ITC[b]	50-90	none	none	none
Wang *et al.* [30]	DMSO/DMF/ CyOH	none	ITC[b]	40-80	none	$\mu\tau=2.8\times10^{-4}$	none
Cheng *et al.* [31]	DMSO/DMF/ CyOH	Choline Bromide	ITC[b]	below 85	0.082	$\tau_1=0.70$ $\tau_2=6.51$	none
Xue *et al.* [32]	DMSO	Bromoacetic acid	ITC[b]	105	0.07	τ=80	none

a LTC: Low-temperature crystallization; b ITC: Inverse temperature crystallization

References

19. Y. Feng, L. Pan, H. Wei, Y. Liu, Z. Ni, J. Zhao, P. N. Rudd, L. R. Cao and J. Huang, J. Mater. Chem. C, 2020, **8**, 11360-11368.20.

23. D. N. Dirin, I. Cherniukh, S. Yakunin, Y. Shynkarenko and M. V. Kovalenko, Chem. Mater., 2016, **28**, 8470-8474.

24. H. Zhang, F. Wang, Y. Lu, Q. Sun, Y. Xu, B. Zhang, W. Jie and M. G. Kanatzidis, J. Mater. Chem. C, 2020, **8**, 1248-1256.

25. Y. Cheng, M. Zhu, F. Wang, R. Bai, J. Yao, W. Jie and Y. Xu, J. Mater. Chem. A, 2021, **9**, 27718-27726.

26. P. Sujith, M. Pratheek, S. R. Parne and P. Predeep, J. Electron. Mater., 2023, **52**, 718-729.

27. L. Gao, J-L. Sun, Q. Li and Q. Yan, ACS Appl. Mater. Interfaces, 2022, **14**, 37904-37915.

28. M. Chen, Y. Yuan, Y. Liu, D. Cao and C. Xu, RSC adv., 2022, **12**, 14838-14843.

29. L. Pan, Z. Liu, C. Welton, V. V. Klepov, J. A. Peters, M. C. De Siena, A. Benadia, I. Pandey, A. Miceli, D. Chung, G. N. M. Reddy, B. W. Wessels and M. G. Kanatzidis, Adv. Mater., 2023, **35**, 2211840.

30. F. Wang, R. Bai, Q. Sun, X. Liu, Y. Cheng, S. Xi, B. Zhang, M. Zhu, S. Jiang, W. Jie and Y. Xu, Chem. Mater., 2022, **34**, 3993-4000.

31. P. Cheng, Z. Liu, R. Kang, J. Zhou, X. Wang, J. Zhao and Z. Zuo, ACS omega, 2023, **8**, 26351-26358.

32. Z. Xue, Y. Wei, H. Li, J. Peng, F. Yao, Y. Liu, S. Wang, Q. Zhou, Q. Lin and Z. Wang, Small, 2023, **19**, 2207588.